POLITECNICO DI TORINO
Repository ISTITUZIONALE

Identification of Waste Materials in Semi-Controlled Test Site Using UAV Thermal and Multispectral Images

Original
Identification of Waste Materials in Semi-Controlled Test Site Using UAV Thermal and Multispectral Images / Makkawi Gassim, H.A., Di Pietra, V., Piras, M.. - X-2/W2-2025:(2025), pp. 133-140. (ISPRS ICWG II/Ia, ICWG I/IV UAV-g 2025 Uncrewed Aerial Vehicles in Geomatics Espoo (Fin) 10-12 Settembre 2025) [10.5194/isprs-annals-x-2-w2-2025-133-2025].

Availability:
This version is available at: 11583/3004817 since: 2025-11-04T17:27:52Z

Publisher:
Copernicus Publications

Published
DOI:10.5194/isprs-annals-x-2-w2-2025-133-2025

Terms of use:

This article is made available under terms and conditions as specified in the corresponding bibliographic description in the repository

Publisher copyright

(Article begins on next page)

01 November 2026

Identification of Waste Materials in Semi-Controlled Test Site Using UAV Thermal and Multispectral Images

Hassan Ali Makkawi Gassim [1], Vincenzo Di Pietra [2], Marco Piras [3]

[1] Dept. of Environmental, Land and Infrastructure Engineering, Politecnico di Torino, 10129, ITALY- hassan.makkawi@polito.it
[2] Dept. of Environmental, Land and Infrastructure Engineering, Politecnico di Torino, 10129, ITALY - vincenzo.dipietra@polito.it
[3] Dept. of Environmental, Land and Infrastructure Engineering, Politecnico di Torino, 10129, ITALY - marco.piras@polito.it

Keywords: waste materials, UAV, thermal images, multispectral images, SCP.

ABSTRACT

The presence of illegal waste materials is one of the most significant challenges for environmental management and human health. Therefore, their identification reduces environmental hazards significantly. Recently, Unmanned Aerial Vehicles (UAVs) equipped with advanced sensors and specialized machine learning algorithms allow for early identification of illegal waste dumping sites. In this scenario, is pivotal to fine-tuning image-based automatic detection and classification procedures with geo-intelligence data obtained in field acquisition campaign conducted in semi-controlled environment. This study aims to identify illegal waste dumping sites by considering the characteristics of waste materials. The testing activities aimed to evaluate a selected list of UAV payload sensors, and the data derived from them, including thermal and multispectral images, to assess their ability to be utilised for automatic waste detection. For this study, the design and testing of a trial site and relative UAV surveying campaign were conducted to mimic the potential presence of waste materials. Regarding the passive thermal response of the surveyed site, a convergence procedure was implemented through R script to calibrate the raw images. Through photogrammetric reconstruction and GNSS-RTK (Global Navigation Satellite System - Network Real Time Kinematic) control point surveying, multiband georeferenced orthomosaic products have been obtained. The calibrated thermal orthophoto was used for the preliminary identification of the waste materials, in particular distinguishing wet sand from dry sand. While the Semi-Automatic Classification Plugin in QGIS was applied to the multispectral orthophoto by utilising materials' spectral signatures to classify the different types of waste materials.

1. INTRODUCTION

Environmental concerns regarding illegal waste sites have increased significantly in several countries (Jiang et al., 2024). Such concerns have been raised due to the hazardous impact on human health and the environmental problems associated with such phenomena (Quesada-Ruiz et al., 2019). Regarding environmental problems, illegal waste sites lead to soil contamination, reduced vegetation cover, air, and water pollution (Limoli et al., 2019). Concerning public health, a study has found an increased risk of stomach, liver, lung, and kidney cancers, as well as ischaemic heart diseases, associated with exposure to illegal waste sites (Fazzo et al., 2023). Besides human health and environmental issues, financial resources are needed to treat illegal waste sites (Seror and Portnov, 2018).

The management of waste materials is typically based on grouping several types of materials that share the same physical and chemical characteristics into a single category. In terms of legislation regarding waste management in Europe, the European Directive amending Directive 2008/98/EC on waste materials imposes certain restrictions. These include a requirement for all Member States to prevent any form of improper and uncontrolled waste disposal. Furthermore, the directive emphasizes that, to enable effective recycling and site treatment operations, waste materials should be collected and dumped according to similar property categories defined by law enforcement, and they should not be mixed (Directive (EU) 2018/851, 2008).

Thus, considering the previously mentioned effects, the early identification of an illegal waste site would lead to several benefits regarding the environment, human health, and minimal financial spending. That said, this study aims to support authorities in identifying illegal waste materials by classifying them based on their characteristics rather than individual items Nowadays, the advanced technology of Unmanned Aerial Vehicles (UAVs) equipped with thermal and multispectral sensors provides effective results with lower cost and high-quality images (Seror and Portnov, 2018; Ahmad and Eisma, 2023; Chio and Lin, 2017). These make the deployment of UAV technology highly effective in detecting waste materials.

2. LITERATURE REVIEW

In this section, the previous studies regarding the use of UAVs thermal and multispectral images in waste materials identification were reviewed. The concerns toward waste management and its impact on the environment and human health have resulted in several active research projects in this area. In addition, the development of remote sensing technologies in recent years, such as the use of UAV technology with its low cost and remarkably efficient thermal and multispectral sensors, enables improving the identification of waste materials by exploiting the spectral response of anthropic materials.

In terms of thermal analysis, Tanda et al. (2020) utilised thermal images captured by UAV and the implementation of heat balance to quantify the methane flow rate to manage urban landfills. The study proposed the detection of biogas depending on distinct thermal prints from the surrounding area generated by anaerobic decomposition and biogas. The study was conducted at two Italian landfills, Mount Scarpino, Genoa, and Scala Erre, Sassari. This approach was effective and less time-consuming compared to ground-based screening tools and sensors for detecting biogas.

Goddijn-Murphy et al. (2022) used a UAV-grade FLIR Vue Pro R 640 thermal camera to detect floating plastic litter, under various environmental conditions. The field results were

confirmed by additional laboratory experiments. The study was performed at Thurso Bay in the Pentland Firth, on the north coast of Scotland. The previous two studies consisted of fundamental concepts that enabled the identification of various waste materials using thermal images collected by UAVs.

In addition to the above-mentioned studies, the study conducted by Jiang et al. (2024) overcame the limitations of DJI thermal images when they were used to create thermal orthophoto. The study proposed a calibration procedure called ThermoSwitcher system based on DJI thermal SDK, which allows for calibrating JPG thermal images to GeoTIFF images. The calibration of thermal images enables heterogeneous temperature distribution without losing temperature information. The study was conducted in Nanjing, China, to identify several land cover types using the surface temperature. The principle of thermal image calibration by converting JPG thermal images using DJI thermal SDK is also applied in our study.

In recent years, the integration of remote sensing technologies and machine learning algorithms has increased significantly, especially for materials and land cover classification. Several studies have used the multispectral images collected by UAVs and machine learning algorithms to classify waste materials.

Oberski et al. (2025) deployed several machine-learning algorithms to classify microplastic waste. The algorithms were implemented on multispectral images from UAV at a waste disposal Plant in northwestern Poland. Several machine learning algorithms were deployed. These include Random Forest, k-nearest neighbour (k-NN), Maximum Likelihood, and Minimum Distance. The accurate result was obtained from k-NN. Also, Cortesi et al. (2022) employed the same concept of UAV multispectral images and machine learning by applying a Random Forest algorithm to detect plastic objects. The study was conducted on the Arno River in Prulli (Reggello, Florence, Italy). The classification results showed high accuracy, with recall and accuracy equal to 98%.

To summarise, several studies have used UAVs thermal and multispectral images to detect and identify the presence of waste materials. These studies relied on surface temperature variation in the case of thermal images and implemented machine learning algorithms on multispectral images for waste materials classification. However, fewer studies have integrated both types of images for waste material identification. This study proposed the integration of a calibrated thermal orthophoto and multispectral orthophoto to identify waste materials. The calibrated thermal orthophoto was used for a preliminary investigation of the waste materials. By deploying R script to convert JPG thermal images to GeoTIFF thermal images. For instance, using calibrated thermal orthophoto allows us to differentiate between dry sand and wet sand relying on surface temperature variation. Then the Random Forest algorithm is applied to classify waste materials. The machine learning classification technique proposed in this study is based on open-source tool Semi-Automatic Classification Plugin in QGIS (Congedo, 2021), which enables simple classification methods without the need for coding expertise.

3. STUDY AREA

This study is strongly enhanced by the design and execution of a semi-controlled test executed at the Calvarina testing ex-military base in Verona, Italy, as shown in Figure 1. Two survey campaigns were executed in October 2023 and, July2024, where several waste materials were distributed to mimic the waste dumping sites.

The waste materials were distributed to mimic the complexity of real waste sites. Therefore, various scenarios were explored, including different land cover types (open area, grassland, tree cover) and types of waste (tyres, wet sand, dry sand, and barrels), as shown in Figure 2.



Figure 1: Showcase site Calvarina, Verona, Italy.



Figure 2: Type of land cover and waste materials.

4. MATERIALS AND METHOD

This study proposes the following methodology, which encompasses two paths. Firstly, a preliminary investigation of the waste materials using a calibrated thermal orthophoto based on the object's surface temperature. Secondly, a machine learning algorithm is applied on multispectral orthophoto by utilising the Semi- Automatic Classification Plugin (SCP) in QGIS software to classify the different types of waste materials based on the object's spectral signature.

In this study, the workflow illustrated in Figure 3 was implemented, including data collection, data processing, analysis, and implementation of the machine learning algorithm.

https://doi.org/10.5194/isprs-annals-X-2-W2-2025-133-2025 | © Author(s) 2025. CC BY 4.0 License.

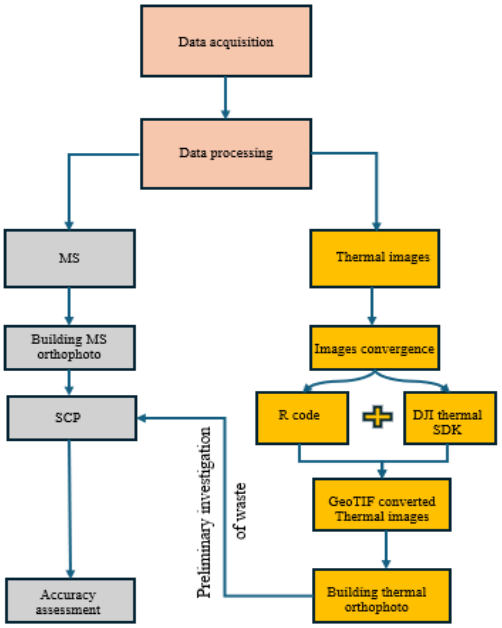


Figure 3: Materials and method workflow.

4.1 Data acquisition (thermal and MS images)

The DJI Mavic M3T was used to collect thermal images. It is equipped with an infrared sensor that operates in the range of 8-14 µm, a resolution of 640x512 pixels, and has a temperature measurement accuracy of ± 2 ºC, which together provide high-quality thermal images. Additionally, the M3T has temperatures measured ranging from -20 ºC to 150 ºC (DJI, 2025a). These highly technical characteristics made M3T ideal for spotting the temperatures of different waste materials. Multispectral images were captured using the DJI Mavic 3M, which has a multispectral camera with four bands: (Green (G): 560 ± 16 nm), (Red (R): 650 ± 16 nm), (Red Edge (RE): 730 ± 16 nm), and (Near-infrared (NIR): 860 nm ± 26 nm) (DJI, 2025b). Both thermal and multispectral images were acquired on the 27th of June 2024 on a sunny day. The difference between the two acquisitions was approximately 1 hour. The flight height was 65.1 m for thermal images and 65.8 m for multispectral images, covering approximately 0.0836 square kilometres. The data obtained from the two acquisitions comprised 201 thermal images and 400 multispectral images.

Moreover, nine artificial targets, Ground Control Points (GCPs), were well distributed in the study area to obtain a georeferenced orthophoto. The coordinates of the GCPs were measured using GNSS technique, implementing NRTK (Network Real Time Kinematic) solutions considering, the reference system WGS 84 / UTM Zone 32N.

4.2 Data processing

Regarding the creation of the calibrated thermal orthophoto, the JPG thermal images captured by DJI Mavic M3T must be converted to GeoTIFF images. To apply this convergence, the R script provided by (Kattenborn and Nelson, 2024) was implemented. The calibration process includes using DJI thermal SDK, creation of GeoTIFF images, and the extraction of metadata from the original images.

Firstly, a radiometric calibration for each image was performed by deploying DJI thermal SDK (dji_irp.exe) (DJI, 2025c). The method encompasses the extraction of 32-bit floating-point temperature values and the use of the following parameters: (distance = 25 m) refers to the distance from the sensor to the targeted objects, (Humidity = 50%) depends merely on the surrounding environment of the site, (Emissivity = 0.95), and (Reflection temperature = 25 ºC) (DJI, 2025c). The parameters used were the default parameters (DJI, 2025c).

Secondly, the ijtiff raster from R packages was used to obtain GeoTIFF images in 32-bit float format using the results obtained from the first step (Kattenborn and Nelson, 2024).

Thirdly, by implementing exifr from R packages, all the necessary EXIF metadata, which includes (GNSS images coordinate, camera settings, focal length, and sensor orientation), were then obtained from the original thermal images and applied to converted GeoTIFF images (Kattenborn and Nelson, 2024). The results obtained from this convergence procedure were GeoTIFF thermal images, where each pixel value represents a real temperature value. These calibrated thermal images are then used to create a calibrated thermal orthophoto covering the entire study area.

The Agisoft Metashape version 2.0.3 was utilised to build the calibrated thermal orthophotos (Agisoft LLC, 2023). The principle of creating the orthophoto in Agisoft Metashape is based on three main concepts: image alignment using aerial triangulation (AT) and bundle block adjustment (BBA), in which the software matches the common images to generate tie points (Agisoft LLC, 2023). The calibrated thermal orthophoto obtained has a GSD of 9.19 cm/pix.

A multi-spectral orthophoto was generated using DJI Terra version 4.1.0 (DJI, 2024d). The result from DJI Terra consists of four orthophotos (green, red, red edge, and NIR) with a GSD of 2.61 cm/pix. These four bands are then imported into QGIS software to be combined into a single orthophoto containing the fourth multi-spectral bands to classify the waste materials using (SCP).

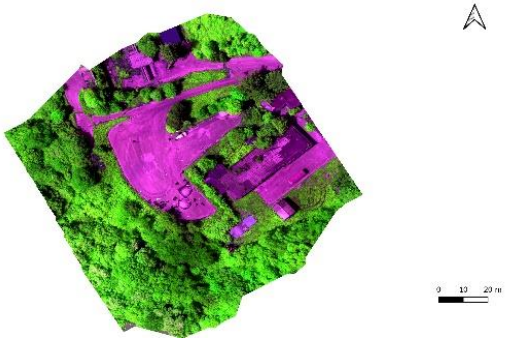


Figure 4: Multispectral orthophoto created using DJI terra.

4.3 Waste materials classification using Random Forest algorithm (SCP) plugin in QGIS

The semi-classification Plugin (SCP) is an open-source plugin introduced by Luca Congedo. SCP aims to provide an automatic tool for raster images to enable land cover classification in a simple way. It uses Remotior Sensus, a Python package that allows imaging processes and GIS data. The SCP uses machine learning algorithms such as Maximum Likelihood, Random Forest, Maximum Distance, and Support Vector Machine

(SVM). This study used Random Forest to classify waste materials (plastic sheets, car tyres, metal barrels, dry sand, and wet sand).

The selection of the Random Forest algorithm is based on the robust and effective results it provides when applied to MS images (Akar and Güngör, 2012; Guo et al., 2022; Iordache et al., 2022). The classification deployed in this study is pixel-based, depending on aggregating classes that share similar chemical characteristics and spectral signatures. Since the classification using Random Forest within the Semi-Automatic Classification Plugin (SCP) is based on the spectral signature, it is ideal for the objectives of this study (Congedo, 2021).

The process of waste materials classification using the Random Forest algorithm within the Semi-Automatic Classification Plugin (SCP) involves several steps. These include band sets definition, training samples, and classification refinement.

To begin with, the band sets were defined considering four MS bands: red, red edge, green, and NIR. Then the centre wavelength for each band was inserted. In addition, a virtual raster was created to obtain a single orthophoto (Congedo, 2021).

Following the band sets, the training samples are created using the region of interest (ROI). ROI are temporary polygons made by the SCP using a region-growing algorithm or drawn manually. The purpose of drawing ROIs is to define the spectral characteristics of the different classes on the multispectral orthophoto. The preliminary investigation provided by the calibrated thermal orthophoto enables better selection for the ROIs. ROIs are then saved as training input with spectral signatures of the exact polygons. Notice that the classification is always based on spectral signatures. The ROIs are defined considering two levels: the first level is the Macro class ID, and the second level, a subset of the Macro class ID, is the class ID level (Congedo, 2021). The following ROIs were defined: pavement, sand, wet sand, metal barrels, tyres, vegetation, plastic sheets, and concrete (see Figure 5).

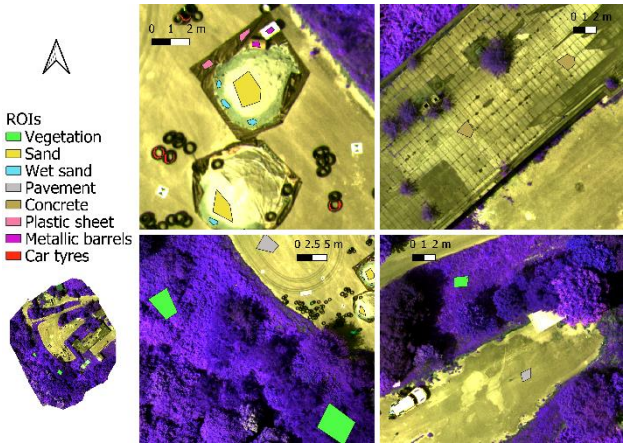


Figure 5: Definition of ROIs in MS orthophoto using SCP.

Once the training samples (ROI) were defined, the first classification was performed using the Random Forest algorithm, considering 60 trees. Also, the cross-validation was deployed, which allows for a data partitioning resampling technique through the cross-validation method. K-fold cross-validation was applied to the training set, which divides the training data into K equally sized folds. Each fold was used as a validation set, while the remaining K-1 folds were used as the training set (Kuhn and Silge, 2022). This approach would increase classification accuracy.

To refine the classification results, the spectral signature for each class was plotted using SCP, as shown in Figure 6. The spectral signature analysis revealed the following: pavement and the concrete of the roof building exhibited similar spectral trends in the NIR band. In addition, plastic sheets and car tyres have shown a closer trend in Red Edge and NIR bands. The band confusion among the different classes is more likely to be linked to similarities in chemical composition between the different classes. Thus, for classification refinement, materials with similar chemical compositions are suggested to be merged into a single class. For instance, plastic sheets and car tyres (polymer class), pavement, and concrete roof buildings (concrete class). Moreover, additional regions of interest were drawn, as shown in Figure 7, for pavement and GCPs as polymer classes to achieve better classification.

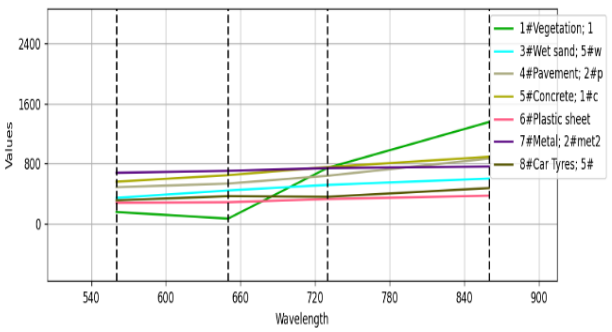


Figure 6: Materials spectral signature in four MS bands using SCP.

In addition to the classes merged, which had previously applied, the increased number of trees was also implemented to enable the algorithm for effective classification. Using 70 trees instead of the 50 trees that were previously applied, the classification accuracy improved significantly.

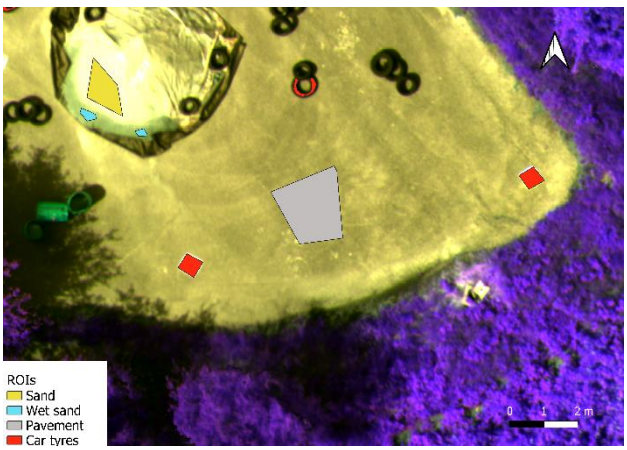


Figure 7: Additional ROIs to refine classification accuracy using SCP.

4.4 Classification accuracy assessment

The accuracy assessment of the Random Forest (RF) classification was made by comparing the polygon test set layers (reference layers). Which were converted into a raster format using the original orthophoto, with the final classified raster. A

This contribution has been peer-reviewed. The double-blind peer-review was conducted on the basis of the full paper.
https://doi.org/10.5194/isprs-annals-X-2-W2-2025-133-2025 | © Author(s) 2025. CC BY 4.0 License.

polygon shapefile containing the field "MC ID" (matching the classification scheme) was added. The MC ID values in the test layers were assigned to match those used during the classification to ensure a valid accuracy assessment. To assess the model's performance, we computed the accuracy assessment metrics for each class, including the user's accuracy (UA), the producer's accuracy (PA), and the Kappa coefficient. Moreover, we computed the overall accuracy and the overall Kappa coefficient (Congedo, 2021).

The calculation of accuracy assessment metrics is based on the area-based error matrix, which enables us to have an unbiased model assessment. The error-based matrix is a cross-tabulation matrix derived from the pixel-based confusion matrix shown in Table 1. The main diagonal of the pixel-based confusion matrix represents the number of pixels from the ground truth correctly classified as class (i) (Olofsson et al., 2014).

	Ground truth				
	Class 1	Class 2	…..	Class k	Total
Class 1	P_{11}	P_{12}	…..	P_{1k}	P_{1+}
Class 2	P_{21}	P_{22}	…..	P_{2k}	P_{2+}
…..	…..	…..	…..	…..	…..
Class k	P_{k1}	P_{k2}	…..	P_{kk}	P_{k+}
Total	P_{+1}	P_{+2}	…..	P_{+k}	n

Table 1: Pixel-based confusion matrix.

To obtain the area-based error matrix, each cell from the pixel-based confusion matrix should be transferred using equation (1).

$$a_{ij} = \frac{P_{ij}}{P_{i+}} w_i \qquad (1)$$

where a_{ij} = area- based error cells
P_{ij} = correctly classified pixels for class (i)
P_{i+} = row total
w_i = the proportion of total raster area as class (i)

	Ground truth				
	Class 1	Class 2	…..	Class k	Total
Class 1	a_{11}	a_{12}	…..	a_{1k}	a_{1+}
Class 2	a_{21}	a_{22}	…..	a_{2k}	a_{2+}
…..	…..	…..	…..	…..	…..
Class k	a_{k1}	a_{k2}	…..	a_{k3}	a_{k+}
Total	a_{+2}	a_{+2}	…..	a_{+k}	n

Table 2: Area-based error matrix.

The accuracy assessment metrics, including the user's and the producer's accuracy for each class as well as the overall accuracy, are then calculated as follows:
As shown in equation (2), the user's accuracy is the ratio between the correct classified samples for class (i) and the row total.

$$U_i = \frac{a_{ii}}{a_{i+}} \qquad (2)$$

The producer's accuracy, as shown in equation (2), is the ratio between the correctly classified samples for class (i) and the total column.

$$P_i = \frac{a_{ii}}{a_{+i}} \qquad (3)$$

The overall accuracy is calculated as shown in equation (4), which is the ratio between the sum of all the classes that are correctly classified in the sample and the total of all samples (n) (Olofsson et al., 2014).

$$O_i = \sum_{i=1}^{k} \frac{a_{ii}}{n} \qquad (4)$$

5. RESULTS AND DISCUSSION

In this section, the results of this study are introduced, starting with a calibrated thermal orthophoto to conduct a preliminary investigation of waste materials. In addition, waste materials classification was obtained using the Random Forest algorithm by deploying SCP on a multispectral orthophoto. The classification was supported by the results from the calibrated thermal orthophoto. The results of the waste classification were obtained by applying the following steps: initial classification, classification enhancement, final classification, and classification accuracy assessment.

5.1 Calibrated thermal orthophoto

The calibrated thermal orthophoto, as shown in Figure 8, was obtained after converting JPG thermal images to GeoTIFF images using the R script. The calibrated orthophoto provides valuable insight for the preliminary investigations of the different types of waste materials.

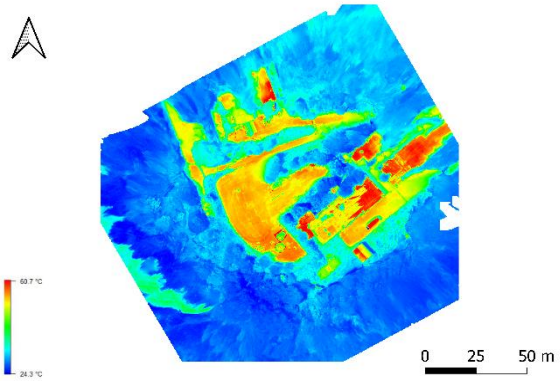


Figure 8: Calibrated thermal orthophoto created using Agisoft Metashape.

As shown in Figure 9, several waste materials were visible based on surface temperature. These include plastic sheets placed below the sand dumping, which can be easily noticed on the pavement due to differences in surface temperature. Dry and wet sand were also visible because wet sand exhibits lower temperature values than dry sand. The calibrated thermal orthophoto allows for other materials to be differentiated, such as metal barrels and car tyres.

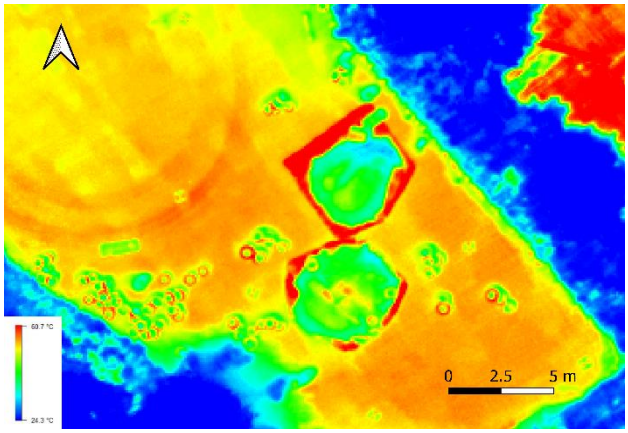


Figure 9: Preliminary investigations using the calibrated thermal orthophoto

5.2 Waste materials classification on MS orthophoto using SCP

5.2.1 Initial classification

Regarding the multispectral classification, eight classes were considered in the initial classification, including vegetation, pavement, concrete, plastic sheet, dry sand, wet sand, car tyres, and metal barrels. As shown in Figure 10, the initial classification provided accurate results regarding vegetation, even for the small vegetation patches on the roof of the building. However, small regions were misclassified due to the presence of shadows. The effect of shaded areas is clearly visible in Figure 10 and 11, where some vegetation and the shaded pavement area were misclassified as car tyres due to the low multispectral reflectance. These are highlighted by the white rectangles in Figure 10 and 11.

Moreover, the algorithm was unable to distinguish between pavement and concrete buildings, as shown by the red rectangles in Figure 10. This misclassification is linked to the similarity in chemical material composition, which leads to similar spectral signatures. Also, the roof membrane was not accurately visible, as shown by the yellow rectangle in Figure 10.

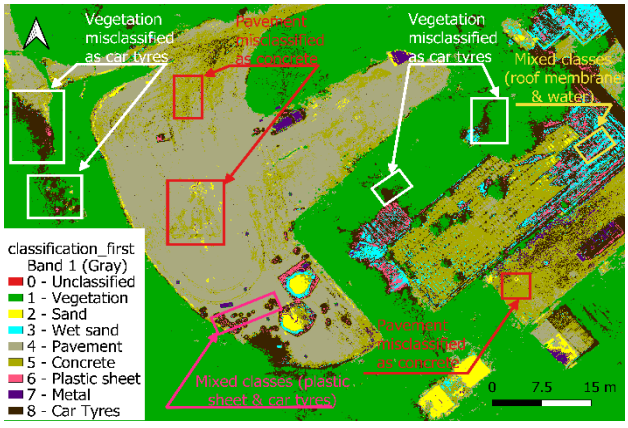


Figure 10: Initial materials classification using Random Forest in SCP.

Figure 11 shows the correct classification of the sand dumps, where wet and dry sand were clearly distinguishable, as were metal barrels. However, mixed class issues were observed in car tyres where plastic sheets class were also assigned to some car tyres as shown by the pink rectangle in Figure 10.

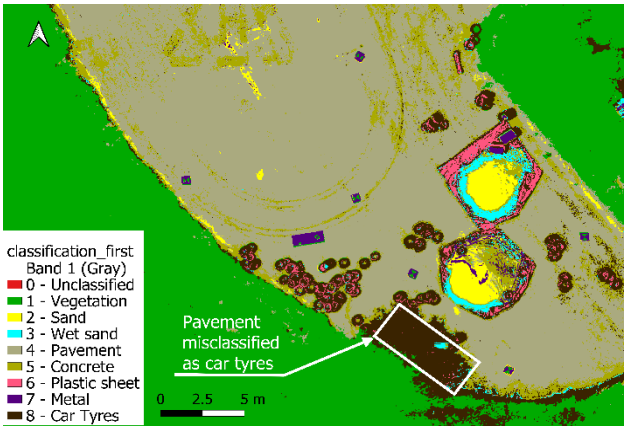


Figure 11: Initial materials classification using Random Forest in SCP

5.2.2 Classification refinement

The inconsistency in some of the classes obtained from the initial classification required further investigation concerning the spectral signature for each class. The classification aims to categorise waste materials based on their similar characteristics. Therefore, the aggregation of classes was implemented based on material characteristics and spectral signature, as explained in the material and method section.

Nevertheless, despite the significant enhancement in the refined classification, the shaded areas still lacked correct classification, which can be considered a limitation for such analysis (see Figure 12 and Figure 13).

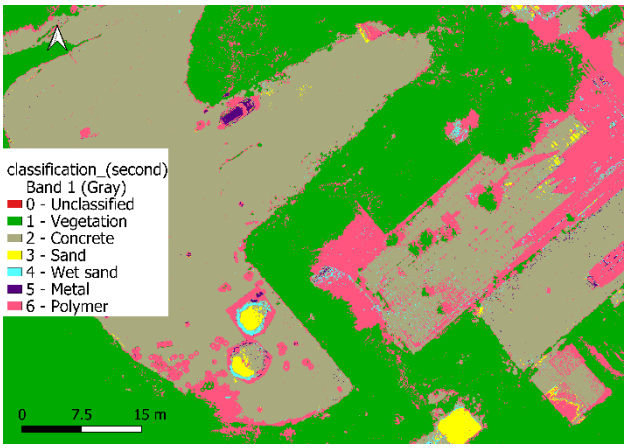


Figure 12: Final materials classification using Random Forest in SCP.

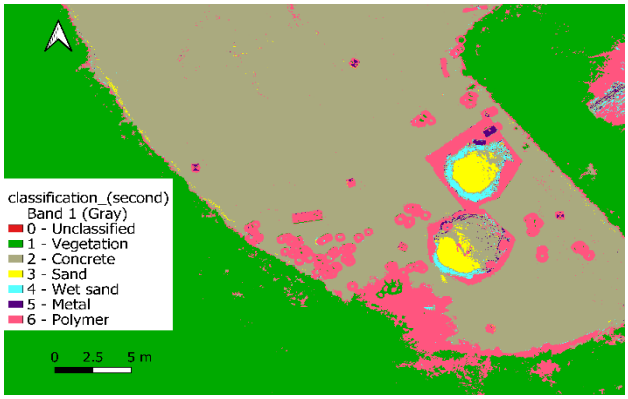


Figure 13: Final materials classification using Random Forest in SCP.

5.2.3 Classification accuracy assessment

The implementation of the classification accuracy assessment was deployed using the reference layers shown in Figure 14. These reference layers represent the ground truth regions selected from the original MS orthophoto. The creation of the reference layers was conducted in accordance with the steps previously explained in Section 4.4. The reference layers were then compared with the final classified raster.

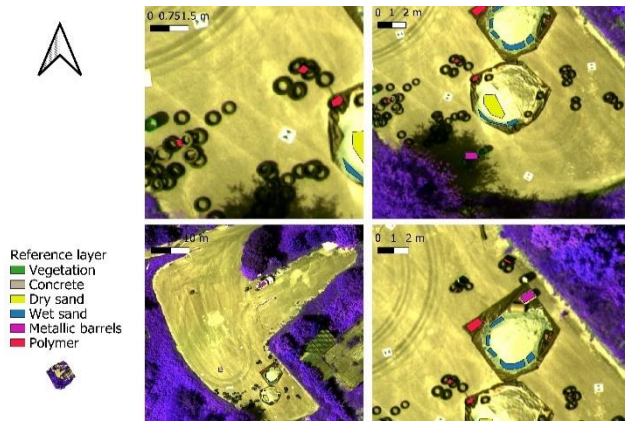


Figure 14: Classification accuracy assessment using SCP

Table 3 illustrates the results obtained from the accuracy assessment using the Semi-Automatic Classification Plugin (SCP) in QGIS. These results include user's accuracy (UA), producer's accuracy (PA), Kappa coefficient, the number of pixels for each reference layer per class (Ref. pixels), and the mapped proportion for each class from the total classified raster (Map prop.). To have a reliable model assessment, the number of reference pixels per class (ground truth) was approximately balanced across classes, as shown in Table 3.

Class	Ref. (pixels)	Map prop.	UA (%)	PA (%)	Kappa
Vegetation	2302	0.8375	98.78	100.00	0.93
Concrete	2307	0.1149	77.07	100.00	0.75
Dry sand	2433	0.0028	99.96	99.34	1.00
Wet sand	2306	0.0027	93.37	9.06	0.93
Metal barrels	2633	0.0006	99.01	3.61	0.99
Polymer	2220	0.0415	62.52	72.53	0.61

Table 3: Accuracy assessment metrics, Kappa coefficient, and weight of each class.

As shown in Table 3, the classification proved reliable results with (98.78% UA, 100% PA) for vegetation, (77.07% UA, 100% PA) for concrete, and (99.96% UA, 99.34% PA) for dry sand. Despite the high user's accuracy that the model achieved for wet sand (93.37%) and metal (99.01%), the model demonstrated lower producer's accuracy for these classes. With (9.06%) for wet sand and (3.61%) for metal. This inconsistency between user's and producer's accuracy is attributed to the rarity of wet sand and metal classes within the entire classified raster when using a balanced number of pixels per class (Stehman, 2012). Additionally, the model shows moderate accuracy metrics for the polymer class, with 63% UA and 73% PA. In general, the overall model performance was 95% for overall accuracy and 0.82 for the Kappa coefficient. These high values for overall accuracy and overall Kappa coefficient demonstrate strong model performance.

6. CONCLUSION

The identification of illegal waste sites is a challenging task worldwide. Nowadays, with advanced technology in remote sensing, such as the use of Unmanned Aerial Vehicles UAVs equipped with advanced sensors, it allows for effective waste detection at a low cost. Moreover, the deployment of machine learning algorithms in remote sensing tasks makes it feasible to identify waste materials. The objectives of this study are based on using thermal and multispectral images captured by UAVs to detect the presence of waste materials, which enables the early identification of illegal waste sites. Such identification provides remarkable benefits for waste management, urban planning, and decision-makers. The methodology implemented in this study encompasses two steps: to have a preliminary waste materials detection using thermal images and then apply open-source tools to classify the waste materials relying on a machine learning algorithm. To enhance the capability of thermal images, this study utilised R script to convert the JPG thermal images to GeoTIFF thermal images in which the value for each pixel represents real surface temperature. The calibrated images are then used to build a calibrated thermal orthophoto, which helps in differentiating different waste materials present on the site. The preliminary investigations provided a fundamental basis to apply machine learning algorithms for classification tasks.
Regarding machine learning classification, this study proposed the use of open-source tools, in particular Semi-Automatic Classification Plugin from QGIS software. The implementation of the Random Forest algorithm on multi spectral orthophoto demonstrated reliable results, particularly when aggregating the waste classes that share the same characteristics and spectral signatures. This approach can enable authorities to achieve effective waste management. Moreover, the model achieved strong performance with an overall accuracy of 95% and a Kappa coefficient of 0.82.

ACKNOWLEDGEMENTS

This work was supported by EMERITUS project, which was funded by the European Union's Horizon Europe research and innovation programme under Grant Agreement No 101073874.

References

Agisoft LLC, 2023. Agisoft Metashape Professional, Version 2.0.3. www.agisoft.com (2023).

Ahmad, J., & Eisma, J. A. (2023). Capturing Small-Scale Surface Temperature Variation across Diverse Urban

Land Uses with a Small Unmanned Aerial Vehicle. Remote Sensing, 15(8), 2042.

Akar, Ö., & Güngör, O. (2012). Classification of multispectral images using Random Forest algorithm. Journal of Geodesy and Geoinformation, 1(2), 105–112.

Chio, S.-H., & Lin, C.-H. (2017). Preliminary Study of UAS Equipped with Thermal Camera for Volcanic Geothermal Monitoring in Taiwan. Sensors, 17(7), 1649.

Congedo, L, 2021. Semi-Automatic Classification Plugin: A Python tool for the download and processing of remote sensing images in QGIS. Journal of Open-Source Software, 6(64), 3172.

Cortesi, I., Masiero, A., Tucci, G., & Topouzelis, K. (2022). UAV-based river plastic detection with a multispectral camera. The International Archives of the Photogrammetry, Remote Sensing and Spatial Information Sciences, XLIII-B3-2022, 855–861.

Directive (EU) 2018/851. (2008). Directive (EU) 2018/851 of the European Parliament and of the Council of 30 May 2018 amending Directive 2008/98/EC on waste. Official Journal of the European Union, L 150, 109–140.

DJI, 2025a. Mavic 3T data sheet. https://enterprise.dji.com/it/mavic-3-enterprise/specs.

DJI, 2025b. Mavic 3M data sheet. https://ag.dji.com/it/mavic-3-m/specs.

DJI, 2025c. DJI Thermal SDK Version 1.7. www.dji.com/it/downloads/softwares/dji-thermal-sdk (2024).

DJI, 2024d. DJI Terra, Version 4.1.0. https://enterprise.dji.com/it/dji-terra/downloads (2024).

Fazzo, L., Manno, V., Iavarone, I., Minelli, G., De Santis, M., Beccaloni, E., Scaini, F., Miotto, E., Airoma, D., & Comba, P. (2023). The health impact of hazardous waste landfills and illegal dumps contaminated sites: An epidemiological study at ecological level in Italian Region. Frontiers in Public Health, 11.

Goddijn-Murphy, L., Williamson, B. J., McIlvenny, J., & Corradi, P. (2022). Using a UAV Thermal Infrared Camera for Monitoring Floating Marine Plastic Litter. Remote Sensing, 14(13), 3179.

Guo, Q., Zhang, J., Guo, S., Ye, Z., Deng, H., Hou, X., & Zhang, H. (2022). Urban Tree Classification Based on Object-Oriented Approach and Random Forest Algorithm Using Unmanned Aerial Vehicle (UAV) Multispectral Imagery. Remote Sensing, 14(16), 3885.

Iordache, M.-D., De Keukelaere, L., Moelans, R., Landuyt, L., Moshtaghi, M., Corradi, P., & Knaeps, E. (2022). Targeting Plastics: Machine Learning Applied to Litter Detection in Aerial Multispectral Images. Remote Sensing, 14(22), 5820.

Jiang, L., Zhao, H., Cao, B., He, W., Yun, Z., & Cheng, C. (2024). A UAV Thermal Imaging Format Conversion System and Its Application in Mosaic Surface Microthermal Environment Analysis. Sensors, 24(19), 6267.

Kuhn and Silge, 2022: Tidy Modeling with R. O'Reilly Media.

Limoli, A., Garzia, E., De Pretto, A., & De Muri, C. (2019). Illegal landfill in Italy (EU)—a multidisciplinary approach. Environmental Forensics, 20(1), 26–38.

Oberski, T., Walendzik, B., & Szejnfeld, M. (2025). The Monitoring of Macro plastic Waste in Selected Environment with UAV and Multispectral Imaging. Sustainability, 17(5), 1997.

Olofsson, P., Foody, G. M., Herold, M., Stehman, S. V., Woodcock, C. E., & Wulder, M. A. (2014). Good practices for estimating area and assessing accuracy of land change. Remote Sensing of Environment, 148, 42–57.

Quesada-Ruiz, L. C., Rodriguez-Galiano, V., & Jordá-Borrell, R. (2019). Characterization and mapping of illegal landfill potential occurrence in the Canary Islands. Waste Management, 85, 506–518.

Seror, N., & Portnov, B. A. (2018). Identifying areas under potential risk of illegal construction and demolition waste dumping using GIS tools. Waste Management, 75, 22–29.

Stehman, S. V. (2012). Impact of sample size allocation when using stratified random sampling to estimate accuracy and area of land-cover change. Remote Sensing Letters, 3(2), 111–120.

T. Kattenborn and D. Nelson, 2024. DJI thermal rpeg to tif (v. 1.0). https://github.com/DanGeospatial/dji_m3t_rpeg_to_tif/blob/main/dji_m3t_rpeg_to_tif_v2.r

Tanda, G., Balsi, M., Fallavollita, P., & Chiarabini, V. (2020). A UAV-Based Thermal-Imaging Approach for the Monitoring of Urban Landfills. Inventions, 5(4), 55.

© 2025. This work is published under https://creativecommons.org/licenses/by/4.0/ (the "License"). Notwithstanding the ProQuest Terms and Conditions, you may use this content in accordance with the terms of the License.